

## Self-interacting dark matter model without dark energy in cosmology

YIXUAN ZHU<sup>1</sup>

<sup>1</sup>*Department of Astronomy, Beijing Normal University. Beijing 100875. PR China*

### ABSTRACT

#### 1. INTRODUCTION

#### 2. THE BASIC EQUATIONS IN THE IDM MODEL

We assume that the total density of the cosmic fluid obeys the collisional Boltzmann equation

$$\dot{\rho} + 3H\rho + \kappa\rho^2 - 2\Psi = 0, \quad (1)$$

where  $\rho$  is the total energy-density of the cosmic fluid, containing dark matter, baryons, and any type of exotic energy,  $\Psi$  is the rate of creation of DM particle pairs, and the annihilation parameter  $\kappa(\geq 0)$  is given by:

$$\kappa = \frac{\langle\sigma u\rangle}{M_x}, \quad (2)$$

where  $\sigma$  is the cross-section for annihilation,  $u$  is the mean particle velocity, and  $M_x$  is the mass of the DM particle. Compared to the usual fluid equation, the effective pressure term is

$$P = \frac{\kappa\rho^2 - \Psi}{3H}. \quad (3)$$

When  $\kappa\rho^2 - \Psi < 0$ , what means that the IDM particle creation term is larger than the annihilation item, IDM may serve as a negative pressure source in the global dynamics of the Universe, like the role of Dark Energy in the general cosmological models.

Basilakos & Plionis (2009) identified two functional forms for which the previous Boltzmann equation can be solved analytically. Referring to Appendix B in Basilakos & Plionis (2009), only one of these two is of interest because it provides a " $\propto a^{-3}$ " dependence of the scale factor, which is

$$\Psi(a) = aH(a)R(a) = C_1(n+3)a^n H(a) + \kappa C_1^2 a^{2m}. \quad (4)$$

And the total energy density is

$$\rho(a) = C_1 a^n + \frac{a^{-3}F(a)}{C_2 - \int_1^a x^{-3}f(x)F(x)dx}, \quad (5)$$

where  $f(a) = -\kappa/[aH(a)]$ , and the kernel function  $F(a)$  has the form

$$F(a) = \exp\left[-2\kappa C_1 \int_1^a \frac{x^{n-1}}{H(x)}dx\right]. \quad (6)$$

The first term of Eq.(5) is the density corresponding to the residual matter creation that results from a possible disequilibrium between the particle creation and annihilation processes, while the second term can be viewed as the energy density of the self-IDM particles that are dominated by the annihilation process.

#### 2.1. Model 1: relation to the $\Lambda$ CDM model

If  $n = 0$ , the global density evolution can be transformed as

$$\rho(a) = C_1 + a^{-3} \frac{e^{-2\kappa C_1(t-t_0)}}{C_2 - \kappa Z(t)}, \quad (7)$$

where  $Z(t) = \int_{t_0}^t a^{-3} e^{-2\kappa C_1(t'-t_0)} dt'$  (Basilakos & Plionis (2009)). Using the usual unit-less  $\Omega$ -like parameterization, we obtain that

$$\left(\frac{H}{H_0}\right)^2 = \Omega_{1,0} + \frac{\Omega_{1,0}\Omega_{2,0}a^{-3}e^{-2\kappa C_1(t-t_0)}}{\Omega_{1,0} + \kappa C_1\Omega_{2,0}Z(t)}, \quad (8)$$

where  $\Omega_{1,0} = 8\pi G C_1 / 3H_0^2$  and  $\Omega_{2,0} = 8\pi G / 3H_0^2 C_2$ , which related to  $\Omega_\Lambda$  and  $\Omega_m$  in the  $\Lambda$ CDM model, respectively. From Eq.(2), we can also give the mass of the DM particle related to the range of  $\kappa C_1$  (in the unit of  $\text{Gyr}^{-1}$ )

$$M_x = \frac{3.325 \times 10^{-12}}{\kappa C_1} \frac{\langle\sigma u\rangle}{10^{-23}} h^2 (1 - \Omega_{2,0}) \text{ GeV}, \quad (9)$$

where  $h \equiv H_0/[100\text{km/s/Mpc}]$ .

#### 2.2. Model 2 : relation to the $w$ CDM model

If  $\kappa = 0$ , the global density evolution can be written as

$$\rho(a) = \mathcal{D}a^{-3} + C_1 a^n, \quad (10)$$

where  $\mathcal{D} = C_2 - C - 1$ . The conditions in which the current model acts as a quintessence cosmology are given by  $\mathcal{D} > 0$ ,  $C_1 > 0$ , and  $w_{\text{IDM}} = -1 - n/3$ . This solution is mathematically equivalent to that of the gravitational matter creation model of(). The Hubble flow is now given by

$$\left(\frac{H}{H_0}\right)^2 = \Omega_{2,0}a^{-3} + \Omega_{1,0}a^n, \quad (11)$$

where  $\Omega_{2,0} = 8\pi G \mathcal{D} / 3H_0^2$  and  $\Omega_{1,0} = 8\pi G C_1 / 3H_0^2$ , respectively.(Basilakos & Plionis (2009))

### 3. DATASET

To constrain the relevant IDM models (Basilakos & Plionis (2009)), we use the newly revised observational  $H(z)$  data (OHD)(Simon et al. (2005); Stern et al. (2010); Moresco et al. (2012); Zhang et al. (2014); Moresco et al. (2016); Ratsimbazafy et al. (2017); Moresco (2015); Borghi et al. (2022); Jiao et al. (2023)), the Pantheon+ set of 1701 SNe Ia (Scolnic et al. (2022)), the QSO data from Lusso, E. et al. (2020), the BAO data from SDSS and DESI 2024.

#### 3.1. The observational $H(z)$ data

It is widely known that the Hubble parameter  $H(z)$  depends on the differential age as a function of redshift  $z$  in the form

$$H(z) = -\frac{1}{1+z} \frac{dz}{dt}, \quad (12)$$

which provides a direct measurement on  $H(z)$  based on  $dz/dt$ . OHD measurements have recently been acquired mainly employing cosmic chronometers (CC). The CC method is used to provide 33 observational data points, which are taken in the redshift range [0.07, 1.965]. The Table 1 lists the OHD dataset used in this analysis. In this case,  $\chi^2$  can be defined as

$$\chi_{\text{OHD}}^2 = \sum_i^{33} \frac{(H_{\text{th}} - H_{\text{data}})^2}{\sigma_i^2}. \quad (13)$$

#### 3.2. Type Ia supernovae

SNe Ia have long been used as "standard candles" to give a direct measurement of their luminosity distance, and provides strong constraints on cosmological parameters. We use the latest Pantheon+ data set of 1701 SNe Ia samples (Scolnic et al. (2022)), which covers the redshift range [0, 2.26].

We use the fiducial SN Ia magnitude ( $M_b$ ) determined from SH0ES 2021 Cepheid host distances (Riess et al. (2022)), which gives the  $\mu_{\text{data}}$  and we give the  $\chi^2$  as

$$\chi_{\text{SNe}}^2 = \Delta^T C^{-1} \Delta, \quad (14)$$

where  $\Delta = (\mu_{\text{th}} - \mu_{\text{data}})$  and  $C^{-1}$  is the inverse of the covariance matrix of the SNe Ia data, the distance modulus is  $\mu = 5 \log_{10}(d_L/\text{Mpc}) + 25$ , and the luminosity distance  $d_L$  can be given as a function of redshift  $z$

$$d_L = (1+z) \int_0^z \frac{cdz'}{H(z')}. \quad (15)$$

To eliminate the advanced restriction to  $H_0$  from  $M_b$ , we adopt the likelihood function as

$$\tilde{\chi}_{\text{SNe}}^2 = \chi_{\text{SNe}}^2 - \frac{B^2}{C} + \ln \left( \frac{C}{2\pi} \right), \quad (16)$$

**Table 1.** The OHD dataset

$z$	$H(z)$	Reference
0.07	69±19.6	Zhang et al. (2014)
0.09	69±12	Simon et al. (2005)
0.12	68.6±26.2	Zhang et al. (2014)
0.17	83±8	Simon et al. (2005)
0.179	75±4	Moresco et al. (2012)
0.199	75±5	Moresco et al. (2012)
0.2	72.9±29.6	Zhang et al. (2014)
0.27	77±14	Simon et al. (2005)
0.28	88.8±36.6	Zhang et al. (2014)
0.352	83±14	Moresco et al. (2012)
0.3802	83±13.5	Moresco et al. (2016)
0.4	95±17	Simon et al. (2005)
0.4004	77±10.2	Moresco et al. (2016)
0.4247	87.1±11.2	Moresco et al. (2016)
0.4497	92.8±12.9	Moresco et al. (2016)
0.47	89±34	Ratsimbazafy et al. (2017)
0.4783	80.9±9	Moresco et al. (2016)
0.48	97±62	Stern et al. (2010)
0.593	104±13	Moresco et al. (2012)
0.68	92±8	Moresco et al. (2012)
0.75	98.8±33.6	Borghi et al. (2022)
0.781	105±12	Moresco et al. (2012)
0.8	113.1±15.1	Jiao et al. (2023)
0.875	125±17	Moresco et al. (2012)
0.88	90±40	Stern et al. (2010)
0.9	117±23	Simon et al. (2005)
1.037	154±20	Moresco et al. (2012)
1.3	168±17	Simon et al. (2005)
1.363	160±33.6	Moresco (2015)
1.43	177±18	Simon et al. (2005)
1.53	140±14	Simon et al. (2005)
1.75	202±40	Simon et al. (2005)
1.965	186.5±50.4	Moresco (2015)

where  $B = \Delta^T C^{-1}$  and  $C$  is the sum of  $C^{-1}$ . Apparently these two functions give the same constraints in  $\Omega_{2,0}$  and  $\log_{10}(\kappa C_1)$ .

#### 3.3. Quasar

The quasar gives a higher redshift than SNe Ia. We use the QSO dataset from Lusso, E. et al. (2020), which gives 2421 samples with the ultraviolet (UV) and X-ray luminosity. The redshift is up to  $\simeq 7.5$ .

The  $L_X - L_{UV}$  relation of quasar is usually written as

$$L_X = \beta + \gamma \log L_{UV}, \quad (17)$$

which gives that

$$\log_{10}(F_X) = \beta + (\gamma - 1) \log_{10}(4\pi) + \gamma \log_{10}(F_{UV}) + 2(\gamma - 1) \log_{10}(d_L), \quad (18)$$

where  $d_L$  is the luminosity distance same as Eq.(15). So the  $\chi^2$  function for the QSO data can be defined as

$$\chi_{\text{QSO}}^2 = \sum_i^{2421} \frac{(y_{\text{th}}^2 - y_{\text{data}}^2)^2}{s_i^2} - \ln(2\pi s_i^2), \quad (19)$$

where  $s_i^2 = dy_i^2 + \gamma^2 dx_i^2 + \delta^2$  refers to the uncertainties on the  $x_i$  ( $\log_{10} F_X$ ) and  $y_i$  ( $\log_{10} F_{UV}$ ) and  $\delta_i$  represent the intrinsic dispersion.

### 3.4. Baryon acoustic oscillation

The Baryon acoustic oscillation method (BAO) provides a key cosmological probe sensitive to the cosmic expansion history with well-controlled systematics. We use two BAO data sets from the SDSS (Alam et al. (2021)) and DESI 2024 (Collaboration et al. (2024)), which are given at Table 2 and Table 3, respectively. The redshift is up to 2.33 both in the SDSS and the DESI 2024 dataset.

The  $\chi^2$  function for the BAO data is defined as

$$\chi_{\text{BAO}}^2 = \sum_i \frac{(D_{\text{th}}/r_d - D_{\text{data}}/r_d)^2}{\sigma_i^2}, \quad (20)$$

where  $D$  refers to  $D_M$ ,  $D_H$ , or  $D_V$ , which are given as

$$D_M(z) = c \int_0^z \frac{dz'}{H(z')}, \quad (21)$$

$$D_H(z) = \frac{c}{H(z)}, \quad (22)$$

$$D_V(z) = [z D_M^2(z) D_H(z)]^{1/3}, \quad (23)$$

and  $r_d$  is the sound horizon at the drag epoch, which is given as

$$r_d = \int_{z_{\text{drag}}}^{\infty} \frac{c_s dz'}{H(z')}. \quad (24)$$

However, the Eq.(8) just have a stiff point when  $z \rightarrow \infty$ , so the IDM model can not give a constraint to the  $r_d$  and we just try to use the cross parameter  $r_d h$  to give the constraints.

## 4. CONSTRAINT RESULTS

We use the Markov chain Monte Carlo (MCMC) method based on the opening package **emcee** to give a global constraints to the free parameters  $\Omega_{2,0}$  and

$\log_{10}(\kappa C_1)$  in Model 1 and  $n$  in Model 2. Besides, we also add the parameter  $H_0$  or  $h$  to give the constraints to the dark matter particle mass  $M_x$ .

The prior range set for free parameters are given at Table 4

**Table 2.** The BAO-only dataset from SDSS

$z_{\text{eff}}$	$D_M/r_d$	$D_H/r_d$	$D_V/r_d$
0.15			$4.47 \pm 0.17$
0.38	$10.23 \pm 0.17$	$25 \pm 0.76$	
0.51	$13.36 \pm 0.21$	$22.33 \pm 0.58$	
0.7	$17.86 \pm 0.33$	$19.33 \pm 0.53$	
0.85			$18.33^{+0.57}_{-0.62}$
1.48	$30.69 \pm 0.8$	$13.26 \pm 0.55$	
2.33	$37.6 \pm 1.9$	$8.93 \pm 0.28$	
2.33	$37.3 \pm 1.7$	$9.08 \pm 0.34$	

**Table 3.** The BAO dataset from DESI 2024

$z_{\text{eff}}$	$D_M/r_d$	$D_H/r_d$	$D_V/r_d$
0.295			$7.93 \pm 0.15$
0.51	$13.62 \pm 0.25$	$20.98 \pm 0.61$	
0.706	$16.85 \pm 0.32$	$20.08 \pm 0.6$	
0.93	$21.71 \pm 0.28$	$17.88 \pm 0.35$	
1.317	$27.79 \pm 0.69$	$13.82 \pm 0.42$	
1.491			$26.07 \pm 0.67$
2.33	$39.71 \pm 0.94$	$8.52 \pm 0.17$	

**Table 4.** Parameters and priors used in analysis

parameter	initial	prior
$\Omega_{2,0}$	0.3	$\mathcal{U}[0.0, 1.0]$
$n$	—	$\mathcal{U}[-10, 10]$
$\log_{10}(\kappa C_1/\text{Gyr}^{-1})$	—	$\mathcal{U}[-10, 0]$
$H_0[\text{km/s/Mpc}]$	70	$\mathcal{U}[60, 80]$
$r_d h[\text{Mpc}]$	100	$\mathcal{U}[50, 150]$
$\beta$	-11	$\mathcal{U}[-15, -5]$
$\gamma$	0.6	$\mathcal{U}[0.0, 1.0]$
$\delta$	0.2	$\mathcal{U}[0.0, 1.0]$

### 4.1. Model 1: mimicking the $\Lambda$ CDM model

The Eq.(8) convergent to the flat  $\Lambda$ CDM model as  $\log_{10}(\kappa C_1) \rightarrow -\infty$ , therefore the constraints could only give the upper limit of what, and give the lower limit of  $M_x$  according to Eq.(9), respectively.

## 5. CONCLUSIONS

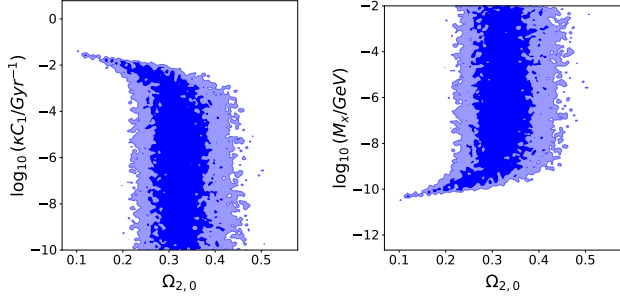


**Figure 1.** The constraint result from the observational  $H(z)$  data

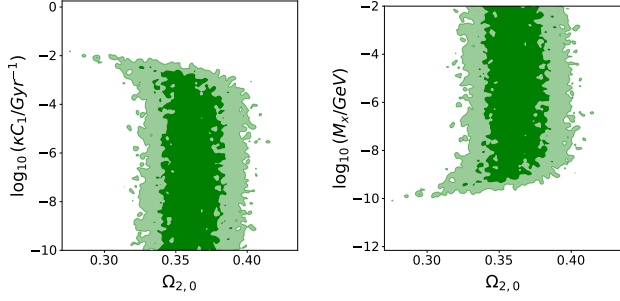


**Figure 2.** The constraint result from the supernovae Ia data

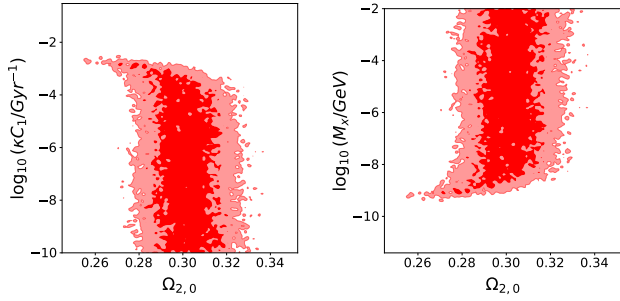


**Figure 3.** The constraint result from the BAO data

## REFERENCES

- Alam, S., Aubert, M., Avila, S., et al. 2021, *Phys. Rev. D*, 103, 083533
- Basilakos, S., & Plionis, M. 2009, *A&A*, 507, 47
- Borghi, N., Moresco, M., & Cimatti, A. 2022, *The Astrophysical Journal Letters*, 928, L4
- Collaboration, D., Adame, A. G., Aguilar, J., et al. 2024, *DESI 2024 VI: Cosmological Constraints from the Measurements of Baryon Acoustic Oscillations*. <https://arxiv.org/abs/2404.03002>
- Jiao, K., Borghi, N., Moresco, M., & Zhang, T.-J. 2023, *The Astrophysical Journal Supplement Series*, 265, 48
- Lusso, E., Risaliti, G., Nardini, E., et al. 2020, *A&A*, 642, A150
- Moresco, M. 2015, *Monthly Notices of the Royal Astronomical Society: Letters*, 450, L16
- Moresco, M., Cimatti, A., Jimenez, R., et al. 2012, *Journal of Cosmology and Astroparticle Physics*, 2012, 006
- Moresco, M., Pozzetti, L., Cimatti, A., et al. 2016, *Journal of Cosmology and Astroparticle Physics*, 2016, 014
- Ratsimbazafy, A. L., Loubser, S. I., Crawford, S. M., et al. 2017, *Monthly Notices of the Royal Astronomical Society*, 467, 3239
- Riess, A. G., Yuan, W., Macri, L. M., et al. 2022, *The Astrophysical Journal Letters*, 934, L7
- Scolnic, D., Brout, D., Carr, A., et al. 2022, *The Astrophysical Journal*, 938, 113

Simon, J., Verde, L., & Jimenez, R. 2005, Phys. Rev. D, 71,

123001

Stern, D., Jimenez, R., Verde, L., Kamionkowski, M., &  
Stanford, S. A. 2010, Journal of Cosmology and  
Astroparticle Physics, 2010, 008

Zhang, C., Zhang, H., Yuan, S., et al. 2014, Research in  
Astronomy and Astrophysics, 14, 1221